JOURNAL OF VIROLOGY, Apr. 2006, p. 3765–3772 Vol. 80, No. 8
0022-538X/06/$08.00+0 doi:10.1128/JVI.80.8.3765–3772.2006

Vpu and Tsg101 Regulate Intracellular Targeting of the Human Immunodeficiency Virus Type 1 Core Protein Precursor Pr55^{gag}

Kirsi Harila,[1,2] Ian Prior,[3] Mathilda Sjöberg,[2] Antti Salminen,[1] Jorma Hinkula,[4] and Maarit Suomalainen[1]*

Department of Virology, Haartman Institute, FIN-00014 University of Helsinki, Finland[1]; The Physiological Laboratory, University of Liverpool, Liverpool L69 3BX, United Kingdom[3]; Department of Biosciences at Novum, Karolinska Institutet, S-141 57 Huddinge, Sweden[2]; and Department of Virology, Swedish Institute for Infectious Disease Control and MTC, Karolinska Institutet, 171 82 Stockholm and Department of Molecular Virology, Linkoping University, 581 83 Linkoping, Sweden[4]

Received 28 September 2005/Accepted 21 January 2006

Assembly of human immunodeficiency virus type 1 (HIV-1) is directed by the viral core protein Pr55^{gag}. Depending on the cell type, Pr55^{gag} accumulates either at the plasma membrane or on late endosomes/multivesicular bodies. Intracellular localization of Pr55^{gag} determines the site of virus assembly, but molecular mechanisms that define cell surface or endosomal targeting of Pr55^{gag} are poorly characterized. We have analyzed targeting of newly synthesized Pr55^{gag} in HeLa H1 cells by pulse-chase studies and subcellular fractionations. Our results indicated that Pr55^{gag} was inserted into the plasma membrane and, when coexpressed with the viral accessory protein Vpu, Pr55^{gag} remained at the plasma membrane and virions assembled at this site. In contrast, Pr55^{gag} expressed in the absence of Vpu was initially inserted into the plasma membrane, but subsequently endocytosed, and virus assembly was partially shifted to internal membranes. This endocytosis of Pr55^{gag} required the host protein Tsg101. These results identified a previously unknown role for Vpu and Tsg101 as regulators for the endocytic uptake of Pr55^{gag} and suggested that the site of HIV-1 assembly is determined by factors that regulate the endocytosis of Pr55^{gag}.

Assembly and budding of human immunodeficiency virus type 1 (HIV-1) is driven by the viral core protein precursor Gag (Pr55^{gag}), which assembles into enveloped virus-like particles (VLPs) when expressed in the absence of other viral proteins (9, 21). Pr55^{gag} is a myristoylated, peripheral membrane protein (3, 9, 14, 40, 47). Concomitantly with assembly and budding, Pr55^{gag} is processed into matrix, capsid (CA), nucleocapsid, and p6 proteins and two smaller peptides SP1 and SP2 by a viral protease present in the minor core component, the Gag-Pol precursor. An intriguing feature of the Pr55^{gag}-mediated assembly of HIV-1 is that different cellular membranes serve as a platform for virus assembly in different cell types. Electron microscopy (EM) and fluorescence microscopy studies have indicated that Pr55^{gag} predominantly accumulates at the plasma membrane, and progeny virions are formed at this site in T cells and model cell lines such as HeLa, 293T, and Cos-1 (see, for example, references 8, 16, and 27), although some Pr55^{gag} has also been identified on late endosomes in these cells (6, 10, 26, 39, 46). In contrast, in macrophages Pr55^{gag} almost exclusively concentrates on late endosomes/multivesicular bodies (MVBs) and progeny virions bud into the lumen of MVBs (25, 28, 31, 33). Egress of virus particles from the cell surface, and probably also from the endosomal assembly sites, is critically dependent on interaction of the Pr55^{gag} p6 domain with the host protein Tsg101 (tumor susceptibility gene 101) (7, 23, 45, 46), which normally functions in formation of MVB vesicles (24). Since ablation of Pr55^{gag}-Tsg101 interactions arrests virus budding at a stage after membrane distortion (7, 46), the primary function of Tsg101 in HIV-1 assembly and budding is thought to be the recruitment of downstream factors essential for the completion of budding and release of virions from the donor membrane (24, 46).

Molecular mechanisms that control cell surface versus endosomal accumulation of Pr55^{gag}, and consequently the choice of virus budding site, are poorly understood. One aspect that remains to be clarified is the route by which Pr55^{gag} reaches its cell surface or endosomal steady-state localization. Like other myristoylated proteins, Pr55^{gag} is expected to be synthesized on cytosolic ribosomes and inserted into membranes posttranslationally (20). It is assumed that the classical endoplasmic reticulum-Golgi secretory route to the plasma membrane and endosomes is not involved in intracellular targeting of Pr55^{gag}, since inhibitors of this transport pathway, such as brefeldin A or monensin, have no effect on the assembly of Pr55^{gag} into extracellular particles (29, 30). Since Pr55^{gag} has been observed on endosomal membranes in a number of different cell types (6, 10, 26, 39, 46), it is possible that the protein is first inserted into endosomal membranes and either retained in these compartments (macrophages) or transported further to the plasma membrane (e.g., HeLa, 293T, or T cells). Alternatively, newly synthesized Pr55^{gag} could be first targeted to the plasma membrane, and endosomal localization could be achieved via endocytosis of the cell surface-associated protein. A third possibility is that a newly synthesized Pr55^{gag} is selectively inserted either into the plasma membrane or endosomal membranes depending on the host cell type.

In the present study, we analyzed targeting of newly synthesized Pr55^{gag} in HeLa H1 cells by pulse-chase studies and a subcellular fractionation assay that efficiently separated plasma

* Corresponding author. Mailing address: Department of Virology, Haartman Institute, P.O. Box 21, FIN-00014 University of Helsinki, Finland. Phone: 358-9-19126688. Fax: 358-9-19126491. E-mail: maarit.suomalainen@helsinki.fi.

membrane from internal membranes. Our results demonstrated that a newly synthesized Pr55^{gag} was initially targeted to the plasma membrane. Pr55^{gag} accumulated at the plasma membrane when coexpressed with the viral accessory protein Vpu but, in the absence of Vpu, a significant fraction of the cell surface-associated Pr55^{gag} proteins was retargeted to internal membranes by endocytosis. This retargeting partially shifted virus assembly from the cell surface to internal membranes. RNA interference (RNAi)-mediated knockdown of Tsg101, or deletion of the p6 domain from Pr55^{gag} suppressed the endocytic uptake of Pr55^{gag} when the protein was expressed in the absence of Vpu. Taken together, these results suggest that the site of HIV-1 assembly is determined by factors that regulate endocytosis of Pr55^{gag}, and the results identified a previously unknown role for Vpu and Tsg101 as regulators of the endocytic uptake of Pr55^{gag}.

MATERIALS AND METHODS

Cell culture and transfection. HeLa H1 cells (American Type Culture Collection) were grown in Dulbecco's modified Eagle medium supplemented with 7% fetal bovine serum (EuroClone) and nonessential amino acids (i.e., HeLa growth medium). 293T cells were cultured as previously described (18). Vesicular stomatitis virus (VSV) G-protein-pseudotyped infectious lentivirus vectors carrying modified HIV-1 genomes were produced by cotransfecting pCMVΔR8.91 and pMD2.VSV.G (generous gifts from Didier Trono [48]), together with a plasmid directing the synthesis of a recombinant HIV-1 genome into 293T cells by a calcium phosphate precipitation technique.

Plasmid constructs. pHXB2D and pNL4-3 were originally obtained from the NIBSC Centralized Facility for AIDS Reagents (the plasmids were donated by Robert Gallo and Mikulas Popovic and by Malcolm Martin, respectively). pHXB2D is a HIV-1 molecular clone with a defective *vpu* gene and truncated *vpr* and *nef* genes (38). Plasmid pHXB2D-Gag is a derivative of pHXB2D that expresses an unprocessed Pr55^{gag} due to an inactivation of the Pol coding region. The plasmid was constructed by replacing the 423-bp ApaI-BclI fragment with a PCR-derived 297-bp ApaI-BclI fragment in which the stop codon of Pr55^{gag} was immediately followed by SmaI and BclI sites. pHXB2D-GagHA and pHXB2D-Gagflag are derivatives of pHXB2D-Gag which express unprocessed Pr55^{gag} proteins that contain hemagglutinin (HA) or FLAG epitopes at their carboxy termini. pNL4-3(Gag), a derivative of pNL4-3 (1), has an inactive Pol-region and expresses an unprocessed Pr55^{gag}. The plasmid was constructed by replacing the 3,779-bp ApaI-SalI fragment with the equivalent ApaI-SalI fragment of pHXB2D-Gag. pNL4-3(Gag/ΔVpu), a derivative of pNL4-3(Gag), has a defective *vpu* gene due to a point mutation in the AUG start codon of *vpu*. The construct was created by replacing the 558-bp SalI-KpnI fragment with the equivalent fragment of pHXB2D. The plasmid pNL4-3(GagΔp6/ΔVpu) encoding a carboxy terminally truncated unprocessed Pr55^{gag} lacking the p6 domain was made from pNL4-3(Gag/ΔVpu) by replacing the 791-bp SpeI-SmaI fragment with a PCR-created 635-bp SpeI-SmaI fragment in which a stop codon and a SmaI site were placed immediately after the last codon of SP2 peptide. pNL4-3(ΔEnv/ΔNef) is a derivative of pNL4-3 with defective *env* and *nef* genes. The first step in construction of pNL4-3(ΔEnv/ΔNef) involved inactivation of the *env* gene on pNL4-3(Gag) by deleting the 580-bp BglII-BglII fragment from the Env coding region. This created the plasmid pNL4-3(Gag/ΔEnv). pNL4-3(ΔEnv/ΔNef) was made by replacing the 2,680-bp SalI-BamHI fragment of pNL4-3-R71.Nef- (35): the plasmid contains an inactivated *nef* gene) with the equivalent fragment from pNL4-3(Gag/ΔEnv). pHXB2D-(ΔVpu/ΔEnv/ΔNef) contains inactive *vpu*, *env*, and *nef* genes. The first step in the construction of pHXB2D-(ΔVpu/ΔEnv/ΔNef) was inactivation of the *env* gene on pHXB2D by deleting a 1,278-bp region between KpnI and BglII sites on *env* which in addition to an internal deletion also introduced a frameshift mutation on the gene. This created the plasmid pHXB2D-(ΔVpu/ΔEnv). pHXB2D-(ΔVpu/ΔEnv/ΔNef) was made from pHXB2D-(ΔVpu/ΔEnv) by inactivating the truncated *nef* gene via converting cohesive ends of XhoI-linearized pHXB2D-(ΔVpu/ΔEnv) into blunt ends by Klenow and subsequently religating the plasmid.

Subcellular fractionations. HeLa H1 cells were seeded on 10-cm plates at a density which gave ~70% confluence after o/n growth. Cells were infected the following day with VSV-G-pseudotyped lentivirus vectors carrying modified HIV-1 genomes. At ~24 h postinfection the now-confluent cell monolayers were metabolically labeled with 50 μCi of [^{35}S]methionine for 30 min (18) and chased for various times in HeLa growth medium containing a 10-fold excess of cold methionine. After the chase, cell monolayers were washed twice with phosphate-buffered saline containing 0.02% EDTA (PBS-EDTA), and the cells were brought into suspension by a 2-min incubation in PBS-EDTA at 37°C. Subsequently, the suspension cells were coated at 4°C with cationic silica beads essentially as previously described (4, 41), except that the coating buffer used was 20 mM 2-[*N*-morpholine]ethanesulfonic acid (pH 6.66 to 6.68) and 150 mM NaCl. After coating, cells were homogenized with a tight-fitting Dounce homogenizer in buffer containing 25 mM HEPES (pH 7.4), 150 mM NaCl, 2 mM $MgCl_2$, 20 μg of phenylmethylsulfonyl fluoride, 1 μg of CLAP (chymostatin, leupeptin, aprotinin, and pepstatin A), and 2.5 mg of heparin per ml (the heparin was included to suppress binding of Pr55^{gag} to chromatin released from broken nuclei). The crude cell homogenates were mixed with 100% Nycodenz solution (AXIS-SHIELD PoC AS) to give a final 60% Nycodenz concentration. The sample (2 ml) was placed on a 1-ml cushion of 70% Nycodenz and overlaid with 1.5 ml of 50% Nycodenz and 0.5 ml of 25 mM HEPES (pH 7.4), 150 mM NaCl, and 1 mM EDTA. The gradient was centrifuged in an SW55 Ti rotor at 63,000 × *g* for 45 min at 4°C. The pellet (i.e., the plasma membrane fraction) was resuspended in hot 0.5% sodium dodecyl sulfate (SDS)–0.5 M NaCl buffer and then boiled for 5 min, and silica beads were removed from the resuspended samples by centrifugation in an Eppendorf centrifuge at full speed for 1 min. The internal membrane fraction at the 50% Nycodenz-buffer interphase was collected and diluted fivefold with 25 mM HEPES (pH 7.4), 150 mM NaCl, and 1 mM EDTA, and membranes were pelleted by centrifugation at 100,000 × *g* for 1 h at 4°C. The internal membrane pellet was solubilized as described above for the plasma membrane, and the samples were diluted with a 10-fold excess of lysis buffer (1% Triton X-100, 25 mM HEPES [pH 7.4], 150 mM NaCl, 1 mM EDTA, 20 μg of phenylmethylsulfonyl fluoride, and 1 μg of CLAP per ml). Pr55^{gag} proteins were immunoprecipitated from the lysates with mouse anti-HIV-1 CA monoclonal antibody 38:9 (17), the Pr55^{gag} processing intermediates and CA with a mixture of monoclonal antibody 38:9 and mouse monoclonal anti-p24 antibody 32/5.17.76 (Abcam, Ltd.), and the HA-tagged Pr55^{gag} with a rabbit polyclonal anti-HA antibody (Sigma).

For biotinylation of the cell surface proteins, HeLa H1 cells were brought into suspension by treatment with PBS-EDTA and incubated in PBS (with $MgCl_2$ and $CaCl_2$) containing 0.5 mg per ml of EZ-Link Sulfo-NHS-SS-biotin (Pierce) for 30 min at 0°C. The sample was quenched with 50 mM NH_4Cl before silica coating. Biotin-tagged proteins in the plasma membrane and the internal membrane fractions were visualized by dot blots using streptavidin-peroxidase polymer (Sigma). Biotin-tagged transferrin proteins (15 μg per ml; Molecular Probes) that had been bound to HeLa H1 cells at 0°C or internalized for 20 min at 37°C in serum-free medium were used as markers for the plasma membrane and recycling endosomes, respectively. In the case of the internalized transferrin, cells were incubated in a pH 4.5 buffer containing 25 mM citric acid, 24 mM trisodiumcitrate, 280 mM sucrose, and 10 μM deferoxamine mesylate for 2 min to remove cell surface-bound transferrin proteins prior to silica coating. Transferrin proteins in the plasma membrane and internal membrane fractions were visualized by Western blotting with streptavidin-peroxidase polymer. The amounts of the endoplasmic reticulum (ER) marker protein calnexin and the late endosome/lysosome marker protein Lamp-1 in the plasma membrane and internal membrane fractions were determined by Western blotting with rabbit polyclonal anti-calnexin (StressGen Biotechnologies Corp.) and goat polyclonal anti-Lamp-1 (C-20; Santa Cruz Biotechnology, Inc.), respectively.

Electron miscroscopy. Cells were fixed at 24 h postinfection with 2% glutaraldehyde in 100 mM HEPES (pH 7.4). The fixed samples were first stained with 1% osmium tetroxide, followed by staining with 0.5% alcoholic uranyl acetate, dehydration in ethanol, and embedding in Agar 100 resin. Sections (60 nm) were cut on an LKB ultramicrotome and imaged in an FEI Tecnai Spirit transmission electron microscope.

RNAi. HeLa H1 cells were seeded on 10-cm plates at a density which gave ~50% confluence after overnight growth. siRNAs directed against the Tsg101 (7) or a control siRNA (GGUCUCUCUUUCGACGUGCdTdT; BLAST searches against the human genome sequence did not identify any target for this siRNA) were transfected into HeLa H1 cells by using Oligofectamine (Invitrogen) in accordance with the manufacturer's instructions. Transfections were carried out in HeLa growth medium containing 7% fetal bovine serum, and 40 μl oligofectamine and 20 pmol siRNA per 10-cm plate were used. Mock-transfected cells were treated with Oligofectamine alone. At about 22 h posttransfection the cells were infected with recombinant lentivirus vectors and then analyzed about 24 h postinfection. The intracellular levels of Tsg101 in mock- and siRNA-treated cells were determined from postnuclear supernatants of cell extracts by Western blotting with a monoclonal anti-Tsg101 antibody (C-2; Santa Cruz

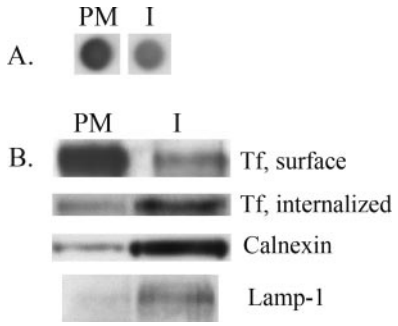

FIG. 1. Coating of HeLa H1 cells with cationic silica beads enables separation of the plasma membrane from internal membranes. HeLa H1 cells were coated with cationic silica beads at 4°C prior to homogenization, and crude cell extracts were fractionated on a Nycodenz step gradient to yield a plasma membrane fraction (PM) and an internal membrane fraction (I). Distribution of marker proteins between PM and I fractions was determined by dot blotting (A) or by Western blotting (B). (A) Plasma membrane-associated proteins were tagged by biotin prior to coating and fractionation, and biotinylated proteins were visualized by streptavidin-peroxidase polymer. (B) Biotin-tagged transferrin proteins bound to cells at 0°C degrees were used as a marker for the plasma membrane (Tf, surface; biotinylated transferrin was visualized by streptavidin-peroxidase polymer). Biotin-tagged transferrin internalized into cells for 20 min at 37°C was used as a marker for recycling endosomes (Tf, internalized). Calnexin and Lamp-1 were used as markers for the ER and late endosomes/lysosomes, respectively.

Biotechnology, Inc.). The monoclonal anti-actin antibody (Chemicon) was used as a control.

RESULTS

Subcellular fractionation method to separate plasma membrane from internal membranes. We have expressed Pr55^{gag} in HeLa H1 cells and analyzed the targeting of the newly synthesized Pr55^{gag} by pulse-chase studies and subcellular fractionations of cell extracts. HeLa H1 cells were chosen since our pilot experiments indicated that Pr55^{gag} can accumulate in these cells either at the plasma membrane or at the internal membranes. Thus, these cells provide a good model system for studying how plasma membrane versus internal localization of the protein is achieved. To determine whether Pr55^{gag} is initially targeted to the plasma membrane or internal membranes requires efficient separation of these membranes. During homogenization, plasma membrane breaks into vesicles and membrane sheets of various density (see, for example, reference 42) that are difficult to separate from, for example, endosomal membranes on conventional sucrose or iodixanol density gradients. Therefore, we chose a fractionation method in which intact cells were coated with cationic silica beads at 4°C prior to homogenization (4, 41), and crude cell extracts were fractionated on a Nycodenz step gradient. The step gradient consisted of a 70% cushion and a 60% sample loading zone overlaid with 50% Nycodenz and buffer solutions. Since the bound silica beads greatly increase density of the plasma membrane, the plasma membrane-derived vesicles and membrane sheets pellet through the 70% Nycodenz cushion during ultracentrifugation (the PM fraction), whereas internal membranes float to the 50% Nycodenz-buffer interphase (I, the internal membrane fraction). Figure 1 shows controls for this fractionation method. In Fig. 1A, externally exposed cell surface-associated proteins were tagged with biotin prior to coating, and biotinylated proteins in the PM and I fractions were visualized by dot blots with horseradish peroxidase-conjugated streptavidin. The majority of biotin-tagged proteins were found in the PM fraction. Similarly, biotin-conjugated transferrin that was bound to cells at 0°C prior to coating was predominantly in the PM fraction (Fig. 1B, Tf surface). In contrast, biotin-conjugated transferrin that had been concentrated into recycling endosomes by internalization at 37°C for 20 min was in the I fraction (Fig. 1B, Tf internalized). The ER protein calnexin, as well as the endosomal/lysosomal marker lysosome-associated membrane protein 1 (Lamp-1), were predominantly in the I fraction (Fig. 1B). Taken together, these results demonstrate that the fractionation method can separate the plasma membrane from internal membranes in HeLa H1 cell extracts.

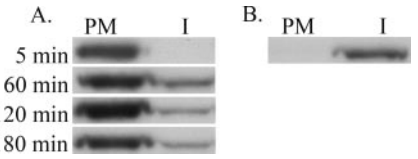

FIG. 2. Newly synthesized Pr55^{gag} is targeted to the plasma membrane and remains at the cell surface when coexpressed with Vpu. (A) NL4-3(Gag)-infected HeLa H1 cells were metabolically labeled with [^{35}S]methionine for 30 min and chased for the indicated times before coating and fractionation of the cell extracts on a Nycodenz step gradient. Pr55^{gag} proteins were immunoprecipitated from the plasma membrane (PM) and internal membrane (I) fractions, and immunoprecipitates were analyzed by SDS-polyacrylamide gel electrophoresis. (B) Distribution of labeled Pr55^{gag} between the PM and I fractions when silica coating was omitted. NL4-3(Gag)-infected cells were metabolically labeled for 210 min and chased for 45 min.

Newly synthesized Pr55^{gag} is inserted into the plasma membrane. To analyze targeting of newly synthesized Pr55^{gag}, HeLa H1 cells were infected with VSV-G-pseudotyped lentivirus vectors carrying modified HIV-1 genomes. At ~24 h postinfection, cells were metabolically labeled with [^{35}S]methionine for 30 min and chased for various times prior to coating and fractionation. Confluent cell monolayers were used in the studies. Amounts of labeled Pr55^{gag} proteins in the PM and I fractions were determined by immunoprecipitation and by SDS-polyacrylamide gel electrophoresis analysis of the immunoprecipitates. Figure 2A shows analysis of newly synthesized, unprocessed Pr55^{gag} expressed from a NL4-3 proviral genome from which the Pol region was deleted [the NL4-3(Gag) genome]. After a 5-min chase, a significant amount of labeled Pr55^{gag} was detected in the PM fraction, but essentially no labeled Pr55^{gag} was present in the I fraction. Similar results were obtained with a 15-min chase (data not shown). Beginning from the 60-min chase point, small amounts of labeled Pr55^{gag} appeared in the I fraction, but the majority of the protein (>80%) was found in the PM fraction at all chase points tested. The NL4-3(Gag) proviral construct efficiently produced VLPs, since large amounts of labeled Pr55^{gag} was found in the culture medium already after 2 h of chase (data not shown). If silica coating was omitted, all labeled Pr55^{gag} was in the I fraction (Fig. 2B), thus confirming that Pr55^{gag} found in the PM fraction in coated cells represented cell surface-associated proteins, and no unspecific protein aggregates. A nonmyristoy-

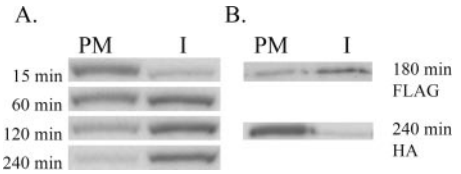

FIG. 3. Newly synthesized Pr55^{gag} is first inserted into the plasma membrane but subsequently endocytosed when expressed in the absence of Vpu. (A) Distribution of newly synthesized Pr55^{gag} proteins between the plasma membrane (PM) and internal membranes (I) at different chase points in NL4-3(Gag/ΔVpu)-infected HeLa H1 cell extracts. Cells were metabolically labeled and analyzed as described in the legend for Fig. 2. (B) Carboxy-terminal HA tag but not FLAG tag inhibits the endocytosis of cell surface-associated Pr55^{gag} expressed in the absence of Vpu. HXB2D-GagHA- and HXB2D-GagFLAG-infected HeLa H1 cells were metabolically labeled for 30 min and chased for the indicated times prior to coating and fractionation.

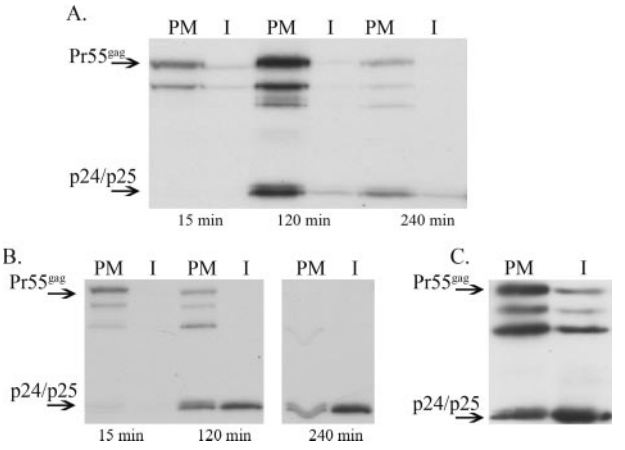

FIG. 4. Vpu inhibits endocytosis of cell surface-associated Pr55^{gag} also when the protein is expressed together with Gag-Pol. (A) Analysis of NL4-3(ΔEnv/ΔNef)-infected HeLa H1 cells. Cells were metabolically labeled and analyzed as described in the legend to Fig. 2. Pr55^{gag} and the p25/p24 CA forms are indicated. Labeled bands between Pr55^{gag} and p25/p24 represent processing intermediates. (B) Analysis of metabolically labeled HXB2D-(ΔVpu/ΔEnv/ΔNef)-infected HeLa H1 cells. (C) Western blot analysis of steady-state distribution of Pr55^{gag} and its processing products between PM and I fractions in HXB2D-(ΔVpu/ΔEnv/ΔNef)-infected cell extracts. The sample was collected at 26 h postinfection.

lated mutant of Pr55^{gag} in which the amino-terminal glycine residue was mutated to alanine failed to associate with either the PM or I fractions (data not shown). Taken together, these results indicated that newly synthesized Pr55^{gag} was inserted into the plasma membrane, and the majority of the proteins remained at the cell surface.

Deletion of the *vpu* gene induces endocytosis of the plasma membrane-associated Pr55^{gag}. We next tested whether localization of Pr55^{gag} to the plasma membrane was an intrinsic property of the protein, or whether other viral proteins had an effect on intracellular targeting of Pr55^{gag}. Elimination of *env* or *nef* genes did not significantly alter the targeting of newly synthesized Pr55^{gag}, i.e., the protein was inserted into the plasma membrane and the majority of labeled Pr55^{gag} remained at the plasma membrane in the absence of Env or Nef expressions (data not shown). In contrast, deletion of the *vpu* gene produced a dramatic change in the intracellular localization of Pr55^{gag}. As shown in Fig. 3A, after a 15-min chase, or 30-min chase (data not shown), the vast majority of labeled Pr55^{gag} was present in the PM fraction in NL4-3(Gag/ΔVpu)-infected cells. Beginning from the 60-min chase point, significant amounts of labeled Pr55^{gag} appeared in the I fraction. By 2 h of chase, ~70% of labeled Pr55^{gag} was shifted to internal membranes. As previously reported for HeLa cells (22), Vpu was also required for efficient virus production from HeLa H1 cells, since NL4-3(Gag)-infected cells produced ~18-fold more VLPs than NL4-3(Gag/ΔVpu)-infected cells (data not shown). Since newly synthesized cytosolic Pr55^{gag} is rapidly targeted to membranes, within 30 min of synthesis (43), the results presented in Fig. 3A suggest that in the absence of Vpu expression Pr55^{gag} is initially targeted to the plasma membrane but is subsequently redistributed to the internal membranes by endocytosis. As shown in Fig. 3B, a carboxy-terminal HA tag, but not a FLAG tag, suppressed endocytosis of cell surface-associated Pr55^{gag}. After 15-min chase, Pr55^{gag}/HA and Pr55^{gag}/FLAG expressed in the absence of Vpu were primarily at the plasma membrane (data not shown) but after 3 h of chase, ~60% of labeled Pr55^{gag}/FLAG had redistributed to internal membranes, whereas >80% of Pr55^{gag}/HA remained at the cell surface even after 4 h of chase.

The effect of Vpu was also tested in the context of Gag and Gag-Pol coexpression. Figure 4A shows an analysis of processed Pr55^{gag} that was expressed from a modified NL4-3 proviral genome lacking *env* and *nef* genes but expressing Vpu [the NL4-3(ΔEnv/ΔNef)]. At all of the time points tested, most of the labeled Pr55^{gag}, its processing intermediates, or the p25/p24 CA forms were found in the PM fraction. Only trace amounts of the proteins could be detected in the I fraction. In contrast, if in addition to the *env* and *nef* genes the *vpu* gene was also deleted [the HXB2D-(ΔVpu/ΔEnv/ΔNef) construct], the intracellular localization of CA forms was changed (Fig. 4B). After 15 min of chase, Pr55^{gag} and two of its early processing intermediates were detected in the PM fraction but not in the I fraction, thus indicating that Pr55^{gag} was first targeted to the plasma membrane. After 2 h of chase, Pr55^{gag} and its early processing intermediates were still found in the PM fraction but, significantly, ~60% of the processed CA forms were in the internal membrane fraction. At the 4-h chase point, only the p25 and p24 CA forms were evident, and the majority of these proteins was found in internal membranes. Although CA was the only Gag form detected in the I fraction in the radioactively labeled samples, Western blot analysis of the PM and I fractions indicated that small amounts of Pr55^{gag} and its processing intermediates were present in internal membranes as well (Fig. 4C). Taken together, the results in Fig. 4 demonstrate that deletion of *vpu* gene induced uptake of plasma membrane-associated core proteins also when Gag and Gag-Pol were coexpressed. These results were confirmed by EM. EM analysis of NL4-3(ΔEnv/ΔNef)-infected cells identified numerous budding profiles at the cell surface (Fig. 5A). Budding profiles were detected at the plasma membrane in HXB2D-(ΔVpu/ΔEnv/ΔNef)-infected cells as well (Fig. 5C), but these cells also contained endosome-like intracellular compartments full of VLP-sized vesicles (Fig. 5B). Occasionally, budding profiles resembling nascent VLPs could be observed on the lim-

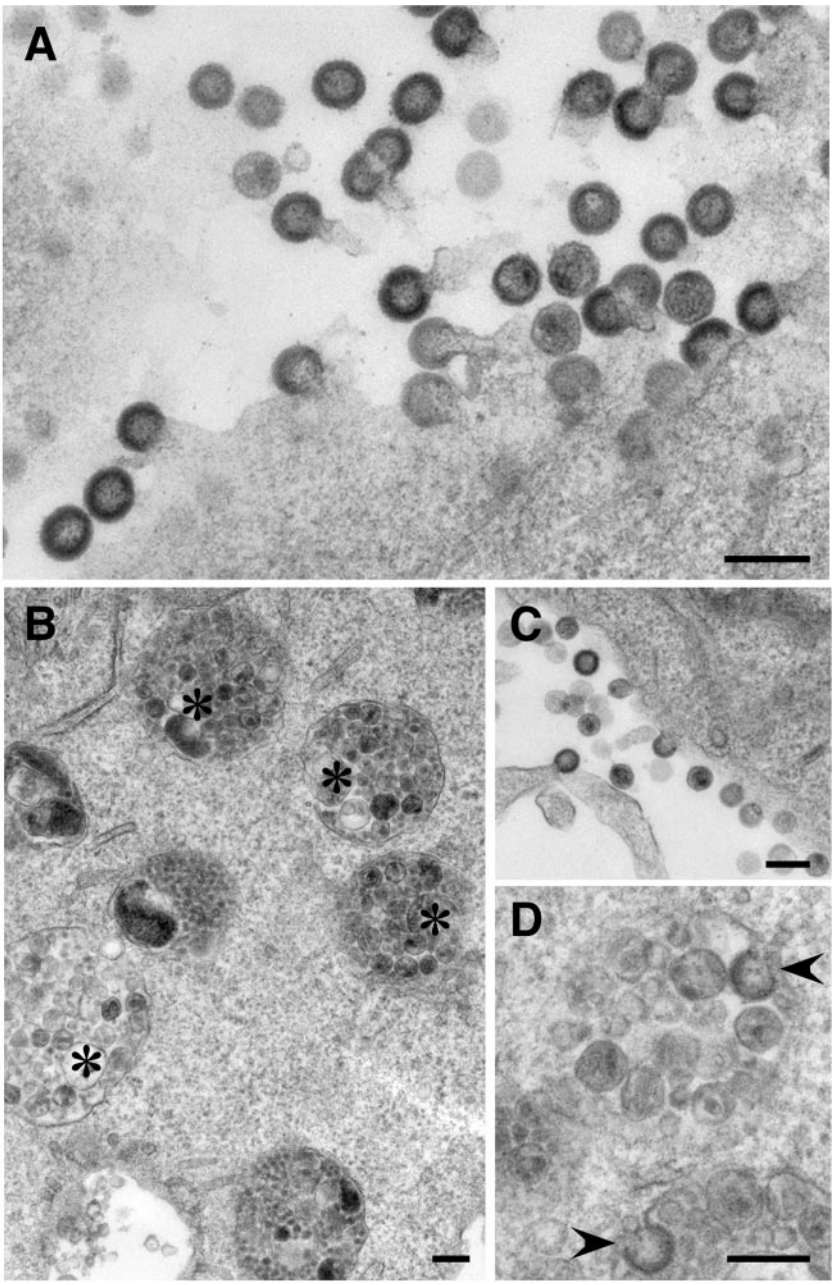

FIG. 5. EM analysis of NL4-3(ΔEnv/ΔNef)- and HXB2D-(ΔVpu/ΔEnv/ΔNef)-infected HeLa H1 cells. (A) NL4-3(ΔEnv/ΔNef)-infected cells. Numerous budding structures are seen at the cell surface. (B to D) HXB2D-(ΔVpu/ΔEnv/ΔNef)-infected cells. In addition to the budding structures at the plasma membrane (C), the cells also contain endosome-like structures (*) full of VLP-sized vesicles (B). (D) Virus-like budding profiles (arrow heads) on the internal VLP-containing compartments. Bar, 200 nm.

iting membrane of these compartments (Fig. 5D). When 10 randomly selected NL4-3(ΔEnv/ΔNef)- and HXB2D-(ΔVpu/ΔEnv/ΔNef)-infected cells, i.e., cells that had budding structures at the cell surface, were scored for VLP-containing endosomal structures, these structures were found in all of the inspected HXB2D-(ΔVpu/ΔEnv/ΔNef)-infected cells. In contrast, only one of the NL4-3(ΔEnv/ΔNef)-infected cells had clearly identifiable endosomal VLPs.

Knockdown of Tsg101 inhibits targeting of Pr55^{gag} to internal membranes. The PTAP motif on the p6 domain of Pr55^{gag} binds Tsg101, and this interaction is necessary for the efficient release of progeny particles (7, 23, 45). We tested the effect of a previously described Tsg101-specific small interfering RNAs (siRNAs) (7) in NL4-3(Gag/ΔVpu)-infected cells to probe whether Tsg101 is involved in endocytosis of Pr55^{gag}. Western blot analysis of cell lysates demonstrated that Tsg101 siRNAs effectively reduced intracellular levels of Tsg101 (Fig. 6A). After a 30-min pulse and 3 h of chase, 58% of labeled Pr55^{gag} remained at the cell surface in Tsg101 siRNA-transfected cells, whereas 73% of labeled Pr55^{gag} was in internal membranes in

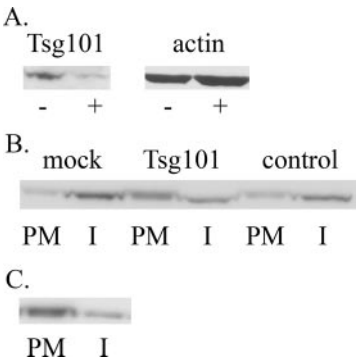

FIG. 6. The p6 domain of Pr55^{gag}, as well as the host protein Tsg101, are required for the endocytic uptake of Pr55^{gag}. (A) Tsg101-siRNAs effectively reduce the intracellular levels of Tsg101. HeLa H1 cells were transfected with Tsg101-specific siRNAs (+) or mock-transfected (−) prior to infection with NL4-3(Gag/ΔVpu) recombinant viruses. Tsg101 levels in postnuclear supernatants were probed by Western blotting, and actin was used as a control to confirm that equal amounts of the two samples were analyzed. (B) HeLa H1 cells were transfected with Tsg101-siRNAs, with control siRNAs of scrambled sequence (control) or mock-transfected (mock) prior to infection with the NL4-3(Gag/ΔVpu) recombinant viruses. Cells were metabolically labeled for 30 min and chased for 3 h prior to silica coating and fractionation. (C) HeLa H1 cells were infected with NL4-3(GagΔp6/ΔVpu) recombinant virus that directs the synthesis of a carboxy-terminally truncated Pr55^{gag} lacking the p6 domain. Cells were metabolically labeled for 30 min and chased for 3 h.

mock-transfected cells (Fig. 6B). Cells transfected with control siRNAs of scrambled sequence had 63% of labeled Pr55^{gag} in internal membranes (Fig. 6B). The less-efficient Pr55^{gag} uptake in Tsg101 siRNA-transfected cells could be due to ablation of Pr55^{gag} interaction with Tsg101, or, alternatively, due to unspecific and/or pleiotropic effects of the Tsg101 siRNAs. To distinguish between these possibilities, we tested uptake of a carboxy-terminally truncated Pr55^{gag} lacking the p6 domain. The truncated protein was expressed from the recombinant proviral genome NL4-3(GagΔp6/ΔVpu). After a 30-min pulse and a 15-min chase, the labeled GagΔp6 protein was in the PM fraction (data not shown). Deletion of the p6 domain inhibited endocytosis of the cell surface-associated protein, since 75% of the truncated proteins were still at the plasma membrane after 3 h of chase (Fig. 6C). Taken together, these results suggest that endocytosis of Pr55^{gag} is critically dependent on interaction of Tsg101 with the p6 domain of Pr55^{gag}.

DISCUSSION

In the present study, we have analyzed targeting of newly synthesized Pr55^{gag} in HeLa H1 cells by pulse-chase studies and by using a subcellular fractionation method that efficiently separates plasma membrane from internal membranes. Our results indicate that Pr55^{gag} is initially targeted to the plasma membrane, and the protein is delivered to internal membranes by endocytosis. Our study also identified Vpu as a key regulator of intracellular targeting of Pr55^{gag}. In the presence of Vpu, the bulk of Pr55^{gag} remained at the plasma membrane after the initial membrane insertion, whereas in the absence of coexpressed Vpu a significant fraction of the cell surface-associated Pr55^{gag} proteins was retargeted to internal membranes. Similar retargeting was observed regardless of whether Pr55^{gag} was expressed as a nonprocessed precursor protein or whether Pr55^{gag} was expressed together with Gag-Pol. These results are in agreement with previous reports indicating that deletion of the *vpu* gene increases virus budding into intracellular compartments in HeLa and T cells (13, 22). We observed a similar increase of VLPs in internal membrane compartments in the absence of Vpu when NL4-3(ΔEnv/ΔNef)- and HXB2D-(ΔVpu/ΔEnv/ΔNef)-infected cells were compared by EM. Furthermore, it is noteworthy that in all of the studies that have identified Pr55^{gag} in internal membranes in transfected or infected, but otherwise nonperturbed HeLa, Cos-1, or 293T cells, the protein was expressed in the absence of Vpu (6, 10, 26, 39). Consistent with our results, Rudner et al. (34) recently identified plasma membrane as the primary target membrane for Pr55^{gag} in HeLa cells. The method used was the fluorescent imaging of cells expressing a tetracysteine-tagged Pr55^{gag} and sequential staining of the cells with two biarsenical compounds that produced different fluorescent signals upon binding to the tetracysteine tag. The dual-labeling procedure enabled the detection of newly synthesized Pr55^{gag}. However, in contrast to our results, the presence or absence of Vpu was reported to have no effect on the association of Pr55^{gag} with the plasma membrane. This discrepancy could perhaps be explained by the carboxy-terminal tetracysteine tag; as exemplified by our HA-tagged Pr55^{gag}, a carboxy-terminal tag can inhibit the endocytosis of cell surface-associated Pr55^{gag}. Since our subcellular fractionation method did not separate internal membrane compartments from each other, the identity of the internal membranes harboring Pr55^{gag} was not established. Fluorescence microscopy analysis of HXB2D-(ΔVpu/ΔEnv/ΔNef)-infected cells indicated a vesicular staining pattern for intracellular Gag (data not shown), but the intracellular Gag-signal in this particular viral genetic background did not extensively colocalize with any of the tested early or late endosomal markers (CD63, Lamp-1, EEA1, or internalized fluorescein isothiocyanate-conjugated transferrin; data not shown).

It is formally possible that the Gag signal in the internal membrane fraction in our silica coating experiments originated from internalized extracellular VLPs rather than from endocytosed plasma membrane-associated Pr55^{gag}. However, we think this is unlikely for the following reasons. First, very little Gag was detected in the internal membrane fraction in NL4-3(Gag)- and NL4-3(ΔEnv/ΔNef)-infected cells despite the fact that these cells released ~18-fold more VLPs than cells expressing the respective ΔVpu-genomes (data not shown). Second, although rare, virus-like budding structures could be identified on internal membrane compartments, and early processing intermediates of Pr55^{gag}, although not as abundant as CA, were observed in internal membrane fraction by Western blotting. Thus, unless VLPs produced in the absence of Vpu have some feature that promotes their rapid uptake after budding from the cell surface, these observations strongly suggest that Gag localization to internal membranes is the consequence of endocytosis of plasma membrane-associated proteins rather than internalization of extracellular VLPs. The mechanism by which Vpu suppresses endocytosis of Pr55^{gag} remains to be elucidated. Since there are no indications that Vpu directly interacts with Pr55^{gag}, Vpu most likely exerts its effect indirectly, e.g., by inducing modifications on the plasma

membrane or by exerting broader modifying effects on the membrane trafficking pathways of the host cell. In order to elucidate how Vpu suppresses endocytosis of Pr55^{gag}, it is essential to understand the molecular basis of endocytosis of Pr55^{gag} when the protein is expressed in the absence of Vpu. Our initial analyses suggest that this uptake requires interactions between the cell surface-associated Pr55^{gag} and Tsg101. siRNAs directed against Tsg101, or deletion of the p6 domain that mediates Pr55^{gag} and Tsg101 interactions (7, 23, 45), inhibited the endocytosis of Pr55^{gag}. siRNAs can cause various off-target effects that are difficult to control for in conventional experimental settings (32, 36), and therefore RNAi-mediated knockdown results have to be interpreted with caution. However, since the endocytosis of Pr55^{gag} was suppressed by deletion of p6 domain, this suggests that the effect of Tsg101 siRNAs was due to ablation of Tsg101 and Pr55^{gag} interactions. Tsg101 was initially identified as being essential for efficient egress of progeny particles from the cell surface assembly sites (7, 23, 45). Tsg101 is a component of the ESCRT-I (endocytic sorting complex required for trafficking) and recruits the so-called class E proteins, which normally function in MVB biogenesis, to the site of HIV-1 assembly and budding (24). The class E proteins also participate in the budding of other retroviruses, filoviruses, and arenaviruses (24). Since HIV-1 assembly is arrested at a late stage (after membrane distortion) when p6-Tsg101 interactions are disrupted (24), it has been assumed that Tsg101 and other class E proteins facilitate the final steps in budding. However, since our results indicate that Tsg101 also has an impact on intracellular localization of Pr55^{gag}, this suggests that the function of Tsg101 in HIV-1 assembly and budding might be more complex than was previously thought.

Several biological activities have been attributed to Vpu (2, 19, 44). One of these is the enhancement of virus release from HIV-1-infected cells. Interestingly, Vpu can also increase virus release from cells infected by other retroviruses (13) and even alphaviruses (11). Since Vpu enhances virus production from most human cells, as well as from human-simian heterokaryons, but not from simian cells, Varthakavi et al. (44) postulated that Vpu counteracts a human cell-specific restriction factor that inhibits HIV-1 particle production. Although our present study by no means excludes the existence of such an assembly/release inhibitor, the data suggest a possible alternative explanation for the Vpu-mediated enhancement of HIV-1 particle release in human cells. Namely, Vpu could affect particle production indirectly via its effects on intracellular targeting of Gag. Since deletion of the *vpu* gene subjected plasma membrane-associated Gag to endocytosis and partially shifted virus assembly to internal membranes, and if these endosomal viruses were only inefficiently released into the extracellular medium, then Vpu-deficient viruses would be expected to produce less extracellular particles than their wild-type counterparts. Vpu has also been reported to enhance overall membrane association of Gag when Gag was expressed from a T7-driven vaccinia virus expression system (5). Although we did not rigorously test the distribution of Gag between cytosolic and membrane fractions in the present study, we, or others (15), have not observed any dramatic reduction in membrane-associated Gag with Vpu-deficient proviral expression systems.

The biological significance of the plasma membrane versus the endosomal assembly of HIV-1 is not fully understood at present, but emerging information suggests that the site of virus assembly could impact HIV-1 pathogenesis. For example, intracellular assembly may promote viral persistence since intracellular virions in macrophages retain infectivity for an extended period of time and can efficiently transfer the infection to lymphocytes upon contact (37). Furthermore, it has been speculated that the cellular site of assembly might have a direct impact on immune recognition and infectivity of the formed virions (12). Thus, understanding the molecular mechanisms that regulate the choice of viral assembly site is important. Our results suggest that cell surface versus internal assembly of HIV-1 in HeLa H1 cells is determined by factors that regulate endocytic uptake of plasma membrane-associated Pr55^{gag}. Our results provide compelling evidence that Vpu promotes cell surface assembly of HIV-1 by inhibiting endocytosis of plasma membrane-associated Pr55^{gag} and that newly synthesized Pr55^{gag} proteins reach internal membrane compartments in HeLa H1 cells via endocytosis from the plasma membrane. The presence of VLPs in internal compartments in HXB2D-(ΔVpu/ΔEnv/ΔNef)-infected cells implies that internalized Pr55^{gag} proteins can engage in productive particle assembly and that the internalization process does not merely represent garbage disposal, i.e., the removal of defective Gag forms from the cell surface. Since HeLa cells recapitulate the main features of HIV-1 assembly in T cells, our results most likely apply to T cells as well. Unfortunately, we could not directly test the targeting of Pr55^{gag} in T cells, since, e.g., Jurkat T cells tended to disrupt during silica coating, and this lead to binding of silica beads to internal membranes as well (data not shown). Whether endocytosis from the plasma membrane is also the mechanism by which Pr55^{gag} is targeted to the MVBs in macrophages is unclear at present, since intracellular targeting of Pr55^{gag} in HeLa H1 cells and macrophages differs at least in two aspects. Namely, Gag is apparently targeted to MVBs in macrophages even when the protein is coexpressed with Vpu (25, 31, 33) and targeting to MVBs in macrophages appears to be independent of Pr55^{gag}-Tsg101 interactions (27). Consequently, either the uptake mechanism is different in macrophages or, alternatively, the initial membrane insertion does not occur at the plasma membrane in these cells. We are currently testing whether the silica coating method can be used to determine the targeting phenotype of newly synthesized Pr55^{gag} in macrophages.

ACKNOWLEDGMENTS

We thank Didier Trono and Kalle Saksela for providing plasmids and Birgitta Lindqvist and Cornelia Muncke for expert technical assistance. Plasmids pHXB2D and pNL4-3 were obtained from the NIBSC Centralized Facility for AIDS Reagents.

This study was supported by grants from Academy of Finland and Swedish Research Council to M.S.

REFERENCES

1. **Adachi, A., H. E. Gendelman, S. Koenig, S. Folks, R. Willey, A. Rabson, and M. A. Martin.** 1986. Production of acquired immunodeficiency syndrome-associated retrovirus in human and nonhuman cells transfected with an infectious molecular retrovirus clone. J. Virol. **59:**284–291.
2. **Bour, S., and K. Strebel.** 2003. The HIV-1 Vpu protein: a multifunctional enhancer of viral particle release. Microbes Infect. **5:**1029–1039.
3. **Bryant, M., and L. Ratner.** 1990. Myristoylation-dependent replication and assembly of human immunodeficiency virus 1. Proc. Natl. Acad. Sci. USA **87:**523–527.
4. **Chaney, L. K., and B. S. Jacobson.** 1983. Coating cells with colloidal silica for high yield isolation of plasma membrane sheets and identification of transmembrane proteins. J. Biol. Chem. **258:**10062–10072.

5. **Deora, A., P. Spearman, and L. Ratner.** 2000. The N-terminal matrix domain of HIV-1 Gag is sufficient but not necessary for viral protein U-mediated enhancement of particle release through a membrane-targeting mechanism. Virology **269:**305–312.
6. **Dong, X., H. Li, A. Derdowski, L. Ding, A. Burnett, X. Chen, T. R. Peters, T. S. Dermody, E. Woodruff, J.-J. Wang, and P. Spearman.** 2005. AP-3 directs the intracellular trafficking of HIV-1 Gag and plays a key role in particle assembly. Cell **120:**663–674.
7. **Garrus, J. E., U. K. von Schwedler, O. W. Pornillos, S. G. Morham, K. H. Zavitz, H. E. Wang, D. A. Wettstein, K. M. Stray, M. Cöte, R. L. Rich, D. G. Myszka, and W. I. Sundquist.** 2001. Tsg101 and the vacuolar protein sorting pathway are essential for HIV-1 budding. Cell **107:**55–65.
8. **Gelderblom, H. R., E. H. S. Hausman, M. Ozel, G. Pauli, and M. A. Koch.** 1987. Fine structure of human immunodeficiency virus (HIV) and immunolocalization of structural proteins. Virol. **156:**171–176.
9. **Gheysen, D., E. Jacobs, F. d. Foresta, C. Thiriart, M. Francotte, D. Thines, and M. D. Wilde.** 1989. Assembly and release of HIV-1 precursor Pr55^{gag} virus-like particles from recombinant baculovirus-infected cells. Cell **59:**103–112.
10. **Goff, A., L. S. Ehrlich, S. N. Cohen, and C. A. Carter.** 2003. Tsg101 control of human immunodeficiency virus type 1 Gag trafficking and release. J. Virol. **77:**9173–9182.
11. **González, M. E., and L. Carrasco.** 2001. Human immunodeficiency virus type 1 Vpu protein affects Sindbis virus glycoprotein processing and enhances membrane permeabilization. Virol. **279:**201–209.
12. **Gould, S. J., A. M. Booth, and J. E. K. Hildreth.** 2003. The Trojan exosome hypothesis. Proc. Natl. Acad. Sci. USA **100:**10592–10597.
13. **Göttlinger, H. G., T. Dorfman, E. A. Cohen, and W. A. Haseltine.** 1993. Vpu protein of human immunodeficiency virus type 1 enhances the release of capsids produced by *gag* gene constructs of widely divergent retroviruses. Proc. Natl. Acad. Sci. USA **90:**7381–7385.
14. **Göttlinger, H. G., J. G. Sodroski, and W. A. Haseltine.** 1989. Role of capsid precursor processing and myristoylation in morphogenesis and infectivity of human immunodeficiency virus type 1. Proc. Natl. Acad. Sci. USA **86:**3195–3199.
15. **Handley, M. A., S. Paddock, A. Dall, and A. T. Panganiban.** 2001. Association of Vpu-binding protein with microtubules and Vpu-dependent redistribution of HIV-1 Gag protein. Virol. **291:**198–207.
16. **Hermida-Matsumoto, L., and M. D. Resh.** 2000. Localization of human immunodeficiency virus type 1 Gag and env at the plasma membrane by confocal imaging. J. Virol. **74:**8670–8679.
17. **Hinkula, J., L. Rosen, V.-A. Sundqvist, T. Stigbrand, and B. Wahren.** 1990. Epitope mapping of the HIV-1 Gag region with monoclonal antibodies. Mol. Immunol. **27:**395–403.
18. **Holm, K., K. Weclewicz, R. Hewson, and M. Suomalainen.** 2003. HIV-1 assembly and lipid rafts: Pr55^{gag} complexes associate with membrane-domains that are largely resistant to Brij 98, but sensitive to Triton X-100. J. Virol. **77:**4805–4817.
19. **Hsu, K., J. Seharaseyon, P. Dong, S. Bour, and E. Marbán.** 2004. Mutual functional destruction of HIV-1 Vpu and host TASK-1 channel. Mol. Cell **14:**259–267.
20. **Johnson, D. R., R. S. Bhatnagar, L. J. Knoll, and J. I. Gordon.** 1994. Genetic and biochemical studies of protein N-myristylation. Annu. Rev. Biochem. **63:**869–914.
21. **Karacostas, V., K. Nagashima, M. A. Gonda, and B. Moss.** 1989. Human immunodeficiency virus-like particles produced by a vaccinia virus expression vector. Proc. Natl. Acad. Sci. USA **86:**8964–8967.
22. **Klimkait, T., K. Strebel, M. D. Hoggan, M. A. Martin, and J. M. Orenstein.** 1990. The human immunodeficiency virus type 1-specific protein Vpu is required for efficient virus maturation and release. J. Virol. **64:**621–629.
23. **Martin-Serrano, J., T. Zang, and P. D. Bieniasz.** 2001. HIV-1 and Ebola virus encode small peptide motifs that recruit Tsg101 to sites of particle assembly to facilitate egress. Nat. Med. **7:**1313–1319.
24. **Morita, E., and W. I. Sundquist.** 2004. Retrovirus budding. Annu. Rev. Cell Dev. Biol. **20:**395–425.
25. **Nguyen, D. H., and J. E. K. Hildreth.** 2000. Evidence for budding of human immunodeficiency virus type 1 selectively from glycolipid-enriched membrane lipid rafts. J. Virol. **74:**3264–3272.
26. **Nydegger, S., M. Foti, A. Derdowski, P. Spearman, and M. Thali.** 2003. HIV-1 egress is gated through late endosomal membranes. Traffic **4:**902–910.
27. **Ono, A., and E. O. Freed.** 2004. Cell-type-dependent targeting of human immunodeficiency virus type 1 assembly to the plasma membrane and the multivesicular body. J. Virol. **78:**1552–1563.
28. **Orenstein, J. M., M. S. Meltzer, T. Phipps, and H. E. Gendelman.** 1988. Cytoplasmic assembly and accumulation of human immunodeficiency virus types 1 and 2 in recombinant human colony-stimulating-factor-1-treated human monocytes: an ultrastructural study. J. Virol. **62:**2578–2586.
29. **Pal, R., R. C. Gallo, and M. G. Sarngadharan.** 1988. Processing of the structural proteins of human immunodeficiency virus type 1 in the presence of monensin and cerulenin. Proc. Natl. Acad. Sci. USA **85:**9283–9286.
30. **Pal, R., S. Mumbauer, G. M. Hoke, A. Takatsuki, and M. G. Sarngadharan.** 1991. Brefeldin A inhibits the processing and secretion of envelope glycoproteins of human immunodeficiency virus type 1. AIDS Res. Hum. Retrovir. **7:**707–712.
31. **Pelchen-Matthews, A., B. Kramer, and M. Marsh.** 2003. Infectious HIV-1 assembles in late endosomes in primary macrophages. J. Cell Biol. **162:**443–455.
32. **Persengiev, S. P., X. Zhu, and M. R. Green.** 2004. Nonspecific, concentration-dependent stimulation and repression of mammalian gene expression by small interfering RNAs (siRNAs). RNA **10:**12–18.
33. **Raposo, G., M. S. Moore, D. Innes, R. Leijendekker, A. Leigh-Brown, P. Benaroch, and H. J. Geuze.** 2002. Human macrophages accumulate HIV-1 particles in MHC II compartments. Traffic **3:**718–729.
34. **Rudner, L., S. Nydegger, L. V. Coren, K. Nagashima, M. Thali, and D. E. Ott.** 2005. Dynamic fluorescent imaging of human immunodeficiency virus type 1 Gag in live cells by biarsenical labeling. J. Virol. **79:**4055–4065.
35. **Saksela, K., G. Cheng, and D. Baltimore.** 1995. Proline-rich (PxxP) motifs in HIV-1 Nef bind SH3 domains of a subset of Src kinases and are required for the enhanced growth of Nef+ viruses but not for down-regulation of CD4. EMBO J. **14:**484–491.
36. **Scacheri, P. C., O. Rozenblatt-Rosen, N. J. Caplen, T. G. Wolfsberg, L. Umayam, J. C. Lee, C. M. Hughes, A. Shanmugam, M. Meyerson, and F. S. Collins.** 2004. Short interfering RNAs can induce unexpected and divergent changes in the levels of untargeted proteins in mammalian cells. Proc. Natl. Acad. Sci. USA **101:**1892–1897.
37. **Sharova, N., S. Swingler, M. Sharkey, and M. Stevenson.** 2005. Macrophages archive HIV-1 virions for dissemination in *trans*. EMBO J. **24:**2481–2489.
38. **Shaw, G. M., B. H. Hahn, S. K. Arya, J. E. Groopman, R. C. Gallo, and F. Wong-Staal.** 1984. Molecular characterization of human T-cell leukemia (lymphotropic) virus type III in the acquired immune deficiency syndrome. Science **226:**1165–1171.
39. **Sherer, N. M., M. J. Lehmann, L. F. Jimenez-Soto, A. Ingmundson, S. M. Horner, G. Cicchetti, P. G. Allen, M. Pypaert, J. M. Cunningman, and W. Mothes.** 2003. Visualization of retroviral replication in living cells reveals budding into multivesicular bodies. Traffic **4:**785–801.
40. **Spearman, P., J.-J. Wang, N. Vander Heyden, and L. Ratner.** 1994. Identification of human immunodeficiency virus type 1 Gag protein domains essential to membrane binding and particle assembly. J. Virol. **68:**3232–3242.
41. **Spector, D. L., R. D. Goldman, and L. A. Leinwand.** 1998. Plasma membrane isolation using the cationic colloidal silica isolation technique, p. 35.1–35.14. *In* Cells: a laboratory manual, vol. 1. Cold Spring Harbor Laboratory Press, New York, N.Y.
42. **Suomalainen, M., K. Hultenby, and H. Garoff.** 1996. Targeting of Moloney murine leukemia virus Gag precursor to the site of virus budding. J. Cell Biol. **135:**1841–1852.
43. **Tritel, M., and M. D. Resh.** 2000. Kinetic analysis of human immunodeficiency virus type 1 assembly reveals the presence of sequential intermediates. J. Virol. **74:**5845–5855.
44. **Varthakavi, V., R. M. Smith, S. P. Bour, K. Strebel, and P. Spearman.** 2003. Viral protein U counteracts a human host cell restriction that inhibits HIV-1 particle production. Proc. Natl. Acad. Sci. USA **100:**15154–15159.
45. **VerPlank, L., F. Bouamr, T. J. LaGrassa, B. Agresta, A. Kikonyogo, J. Leis, and C. A. Carter.** 2001. Tsg101, a homologue of ubiquitin-conjugating (E2) enzymes, binds the L domain in HIV type 1 Pr55Gag. Proc. Natl. Acad. Sci. USA **98:**7724–7729.
46. **von Schwedler, U. K., M. Stuchell, B. Muller, D. W. Ward, H.-Y. Chung, E. Morita, H. E. Wang, T. Davis, G.-P. He, D. M. Cimbora, A. Scott, H.-G. Kräusslich, J. Kaplan, S. G. Morham, and W. I. Sundquist.** 2003. The protein network of HIV budding. Cell **114:**701–713.
47. **Zhou, W., L. J. Parent, J. W. Wills, and M. Resh.** 1994. Identification of a membrane-binding domain within the amino-terminal region of human immunodeficiency virus type 1 Gag protein which interacts with acidic phospholipids. J. Virol. **68:**2556–2569.
48. **Zufferey, R., D. Nagy, R. J. Mandel, L. Naldini, and D. Trono.** 1997. Multiply attenuated lentiviral vector achieves efficient gene delivery in vivo. Nat. Biotechnol. **15:**871–875.